Supplementary Materials

Supplementary files:
Five supplementary files are available with this manuscript.

1. Detailed location maps
    Location maps for each of the five terranes in this study showing the locations where GRS measurements were taken.
2. Methods
    An explanation of the methods used for data collection and processing.
3. Comparison of GRS and XRF measurements
    Tables comparing the average concentrations of K–U–Th in subsolidus protolith and suprasolidus residual granulite-facies rocks from the GRS devices and conventional XRF.
4. Sample locations and heat producing element concentrations.
    A list of the K–U–Th concentrations that were sampled by the GRS devices for each terrane and their respective GPS coordinates.
5. Heat production rate calculations
    Values used for the calculation of the heat production rates of each terrane in this study. Subsolidus calculations are highlighted in blue (in the left column) and are at the top of each tab, whereas suprasolidus calculations are highlighted in red and are at the bottom of each tab. The K_2O (wt%), U (ppm) and Th (ppm) columns on the left are the values detected by the GRS devices, as listed in the previous supplementary file. All calculations are done at 0 Ma (their current heat production). Errors from the manufacturer were used to calculate the upper and lower bounds of the concentration of each element. The final heat production value and its 1 sigma error are listed in the two right columns.

METHODS

Gamma Ray Spectrometer (GRS) Devices

All data used in this study were collected in situ using Radiation Solutions portable gamma ray spectrometer (GRS) devices (RS-230 and RS-330 models). The RS-230 models have a 103 cm^3 bismuth germinate oxide crystal sensor whereas the RS-330 has a 344 cm^3 sodium-iodide detector. The units were calibrated using concrete test pads, constructed by Radiation Solutions. The detectors housing the sensors were placed directly onto the outcrop and counts of K, U and Th were obtained over 120 seconds. The detectors collect data from a volume of ~0.5 m^3, so only outcrops larger than this size were used. The outcrops that were chosen were the least weathered wherever possible. The uncertainties were calculated according to the manufacturer's specifications (Supplementary data). The different crystal sensors in the two models resulted in differences in their abilities to detect U and distinguish it from K and Th. This resulted in the overestimation of U concentrations in data collected from the RS-230 models. All of the data collected from the RS-230 models were normalized to the values from the RS-330 model, as the larger crystal in the RS-330 allows for more accurate determination of HPE concentrations. As a result, the U concentrations in the readings from the RS-230 GRS devices were lowered, but K and Th values remained the same. As the present study seeks to compare the HPE concentrations between subsolidus and suprasolidus rocks, the absolute values, while important, are secondary to the comparative concentration differences between subsolidus and suprasolidus conditions. The concentrations of K–U–Th collected by GRS in this study are in reasonably good agreement with whole-rock compositions determined by XRF for comparison. A comparison of average XRF and GRS K–U–Th is given in the supplementary data. However, given that the GRS devices sample a larger volume than can be practically sampled via conventional geochemical analysis, it is not surprising that there are some differences between the two

different sampling methods. U and Th are concentrated primarily within accessory minerals, which are not solely controlled by major element bulk composition. This results in an non-uniform distribution of U and Th throughout the protolith, meaning that their concentrations may vary on the scale of a hand sample to an outcrop (Jaupart and Mareschal, 2005; Bea, 1996), resulting in different concentrations being present in small conventional geochemical samples and the 0.5 m^3 volume sampled by the GRS units. Importantly, the GRS units are internally consistent and allow collection of large data sets that would be logistically and financially impractical to collect using conventional analytical methods. However, due to the large sample volume collected by the GRS devices, precision sampling was not able to be achieved in migmatitic rocks. As a result, rocks in which melt had segregated, but not yet left the residue were sampled as a whole, rather than just obtaining samples of the residual material.
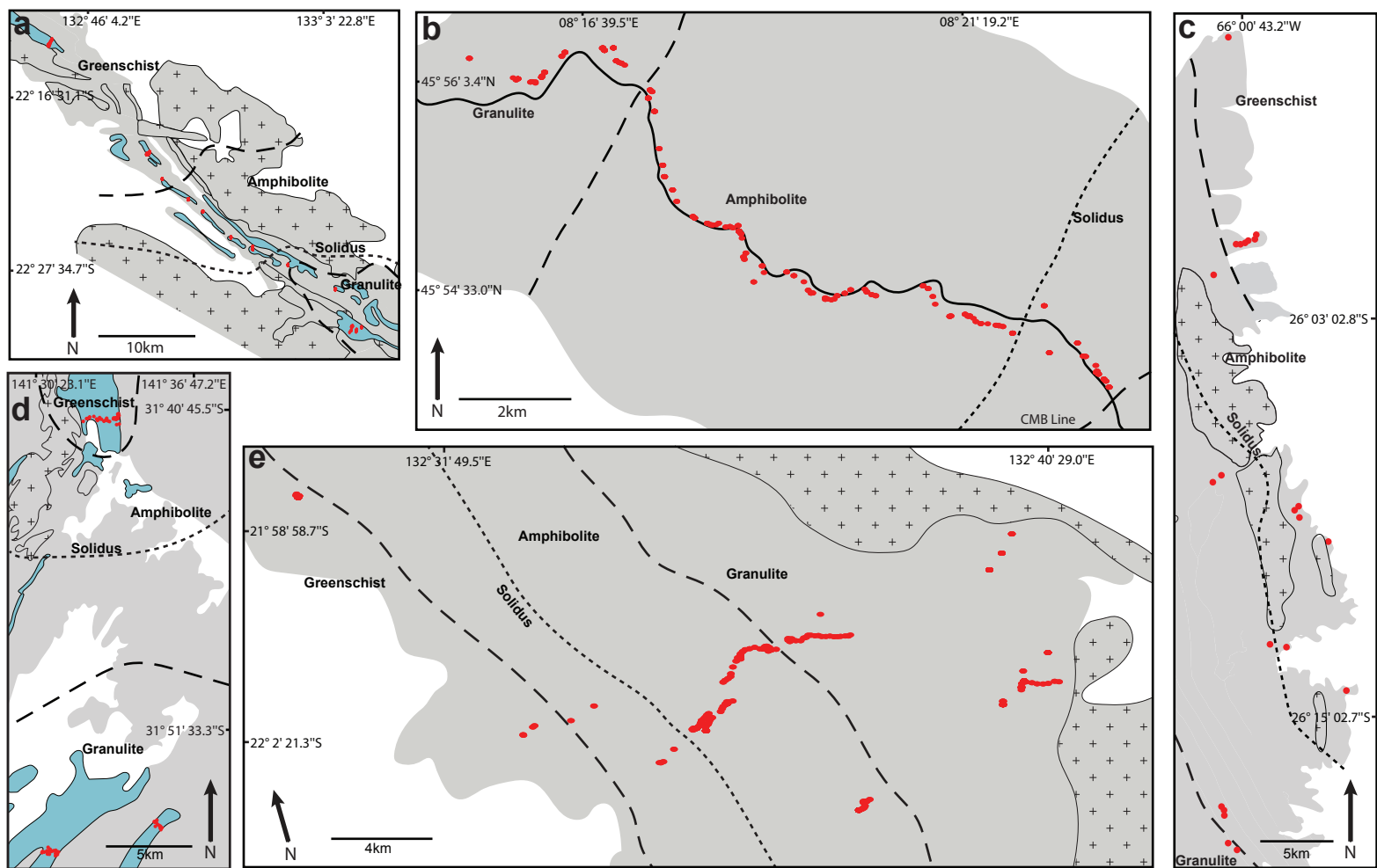
Figure DR1. Location maps of the five terranes used in this study; (a) the Reynolds Range, (b) the Ivrea-Verbano Zone, (c) Sierra de Quilmes, (d) Broken Hill and (e) Mt Stafford. The red circles mark the locations where GRS measurements were taken. Long dashed lines represent changes in metamorphic facies and short dashed lines represent the solidus in each location. Crosses represent granites and, where applicable, blue units mark the particular lithology that was followed. Modified from (a) Morrissey et al. (2014), (b) Redler et al. (2013), (c) Büttner et al. (2005), (d) Willis (1989) and (e) White et al. (2003).